frontiers | Frontiers in Energy Research

TYPE Original Research
PUBLISHED 05 September 2023
DOI 10.3389/fenrg.2023.1272132

OPEN ACCESS

EDITED BY
Peng Tan,
CNPC Engineering Technology R&D Company Limited, China

REVIEWED BY
Qitao Zhang,
The Pennsylvania State University (PSU), United States
Yi Zhang,
Dalian University of Technology, China

*CORRESPONDENCE
Debin Kong,
kongdb@ustb.edu.cn
Wenning Zhou,
wenningzhou@ustb.edu.cn

RECEIVED 03 August 2023
ACCEPTED 24 August 2023
PUBLISHED 05 September 2023

CITATION
Kong D, Meng X, Zhu J and Zhou W (2023), Molecular dynamics simulation of surfactant induced wettability alteration of shale reservoirs.
Front. Energy Res. 11:1272132.
doi: 10.3389/fenrg.2023.1272132

Molecular dynamics simulation of surfactant induced wettability alteration of shale reservoirs

Debin Kong[1,2]*, Xianglong Meng[1,3], Jiadan Zhu[4] and Wenning Zhou[4]*

[1]State Key Laboratory of Shale Oil and Gas Enrichment Mechanisms and Effective Development, Beijing, China, [2]School of Civil and Resources Engineering, University of Science and Technology Beijing, Beijing, China, [3]Research Institute of Exploration and Production, Beijing, China, [4]School of Energy and Environmental Engineering, University of Science and Technology Beijing, Beijing, China

Shale oil has recently received considerable attention as a promising energy source due to its substantial reserves. However, the recovery of shale oil presents numerous challenges due to the low-porosity and low-permeability characteristics of shale reservoirs. To tackle this challenge, the introduction of surfactants capable of modifying wettability has been employed to enhance shale oil recovery. In this study, we perform molecular dynamics simulations to investigate the influence of surfactants on the alteration of wettability in shale reservoirs. Firstly, surfaces of kaolinite, graphene, and kerogen are constructed to represent the inorganic and organic constituents of shale reservoirs. The impact and underlying mechanisms of two types of ionic surfactants, namely, the anionic surfactant sodium dodecylbenzene sulfonate (SDBS) and cationic surfactant dodecyltrimethylammonium bromide (DTAB), on the wettability between oil droplets and surfaces are investigated. The wettability are analyzed from different aspects, including contact angle, centroid ordinates, and self-diffusion coefficient. Simulation results show that the presence of surfactants can modify the wetting characteristics of crude oil within shale reservoirs. Notably, a reversal of wettability has been observed for oil-wet kaolinite surfaces. As for kerogen surfaces, it is found that an optimal surfactant concentration exists, beyond which the further addition of surfactant may not enhance the efficiency of wettability alteration.

KEYWORDS

shale oil, surfactant, wettability alteration, enhanced oil recovery, molecular dynamics simulation

1 Introduction

With the rapid advancement of society and economy, traditional oil and gas resources cannot meet the increasing demand (Zheng et al., 2022; Sun et al., 2023). Hence, it is of great significance to enhance oil and gas production through advanced technologies. Despite recent great breakthroughs in untraditional oil exploration, a substantial amount of shale oil remains trapped within shale reservoirs due to their low-porosity and low-permeability characteristics, resulting in relatively low recovery rates (Zou et al., 2019; Tang et al., 2020; Sun C. et al., 2021). During oil extraction operations, residual oil gets trapped in the nanopores of shale reservoirs after water injection, presenting a significant challenge to the oil recovery process (Dang et al., 2022; Guo et al., 2022). In recent years, several enhanced oil recovery (EOR) techniques have been developed (Rezaei et al., 2018; Zhao et al., 2021; Yang

et al., 2023), with surfactant flooding emerging as one of the most effective technologies for oil recovery enhancement (Liu et al., 2019a; Sun Y.-P. et al., 2021; Larestani et al., 2022). Surfactants exhibit diverse and unique physical and chemical properties, thereby offering considerable potential for optimizing oil recovery under varying conditions, including geological conditions, reservoir compositions, brine salinities, etc. (Tang et al., 2019)

From a macroscopic perspective, the deformability and mobility of oil droplets play a crucial role in determining the ease of detaching oil droplets from the rock surface of oil reservoirs, ultimately leading to enhanced oil recovery (Zhang et al., 2010; Pei et al., 2012). A Previous researchers have conducted extensive experimental and theoretical studies, which have elucidated two primary mechanisms through which surfactants enhance oil recovery. Firstly, surfactants reduce the interfacial tension between oil and water, thereby improving the fluidity of crude oil (Liu et al., 2022; Zhou et al., 2022). Secondly, they alter the wettability of reservoirs from lipophilic to hydrophilic, facilitating the release of more residual oil and enhancing oil recovery (Mirchi et al., 2015; Kubelka et al., 2021; Okunade et al., 2021). Currently, research on the influence of different wettability conditions on the adsorption and diffusion behaviors of shale reservoirs is still in its early stages. Scholars hold different views on shale wettability due to differences in tectonic features and mineral compositions. Shale surface wettability is a critical factor in shale oil recovery as it directly affects the distribution of oil within shale reservoirs, the injection of oil displacement agents into the formation, and the effectiveness of oil displacement (Zhao and Jin, 2021; Shi et al., 2022).

The wettability of reservoir rocks can be influenced by external conditions. Despite extensive research efforts made by scholars worldwide to understand the mechanisms underlying reservoir wettability, a consensus has not yet been reached. Since reservoir rocks are formed in water environments, most of the component minerals are hydrophilic (Guo et al., 2012). Consequently, the initial state of the reservoir rock surface is hydrophilic, characterized by the presence of a water film on the surface. However, the generation and migration of oil and gas within the reservoir typically result in a transition from hydrophilic to lipophilic wettability (Su et al., 2018; Zhang et al., 2020). Furthermore, the wettability of reservoirs can be further modified by drilling fluids and various oil displacement agents such as water, chemicals, and CO_2 (Al Mahrouqi et al., 2017; Yao et al., 2021; Deng et al., 2020; Zhang et al., 2022; Afekare et al., 2021; Qin et al. 2022). These modifications in wettability are often desirable since altering the distribution of reservoir fluids within the pore network through the introduction of oil displacement agents can enhance shale oil recovery.

Researchers have conducted experimental investigations to study the impact of surfactants on enhancing shale oil recovery. Mirchi et al. (Mirchi et al., 2015) investigated the dynamic interfacial tensions and contact angles in two brine/oil/shale systems in the presence of surfactants using the rising/captive bubble technique. They reported that anionic surfactants exhibit higher adsorption on shale compared to nonionic surfactants. SalahEldin Hussien et al. (SalahEldin Hussien et al., 2019) studied the effects of surfactants on fracturing fluid performance by measuring surface tension using the pendant drop technique. Their results revealed that surfactants significantly influenced the wettability of shale rock, rendering it more water-wet. Liu et al. (Liu et al., 2019b) utilized nuclear magnetic resonance (NMR) to evaluate the wettability of shales. Their results indicated that anionic surfactants are more effective compared to nonionic and cationic surfactants in altering the wettability of clay surfaces. Although certain quantitative results can be obtained, it remains challenging to observe the underlying mechanisms and microscopic processes solely through macroscopic experiments (Roshan et al., 2016).

With the rapid development of computer technology, molecular dynamic (MD) simulation is becoming an effective tool for unravelling the underlying mechanisms governing complex processes and behaviors at the microscale level (Zhou et al., 2019a; Zhou et al., 2019b; Zhou et al., 2020; Chen et al., 2023). Researchers have applied extensive MD simulations on investigating the wettability behaviors of shale reservoir for EOR. Chai et al. (2009) examined the wettabilities of surfaces of hydroxylated and silylated amorphous silica. They claimed that the fully silylated silica surface

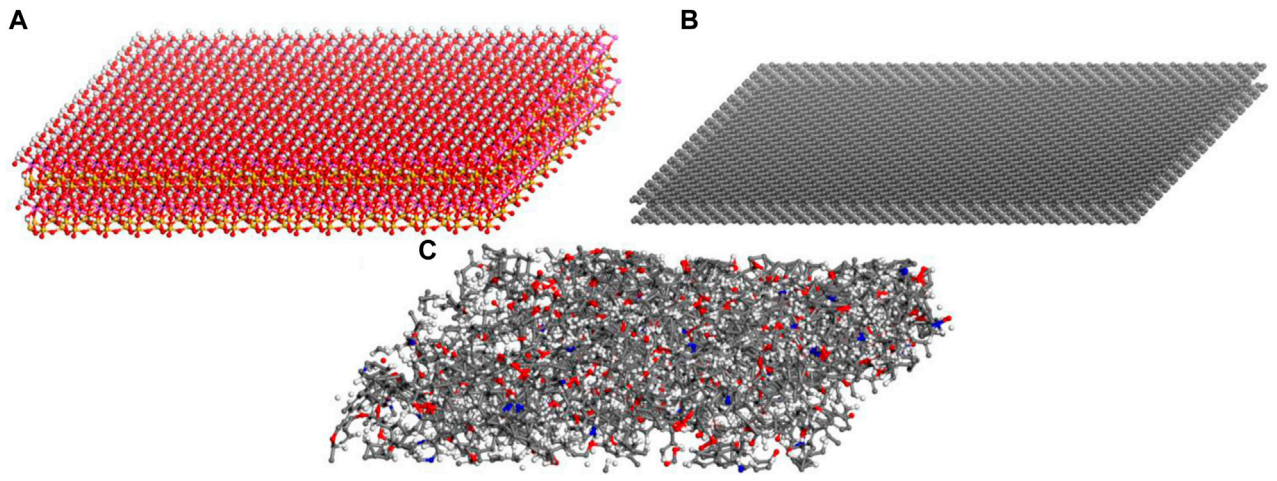

FIGURE 1
Different surface models: **(A)** kaolinite; **(B)** graphene; **(C)** kerogen. Red, white, yellow, purple, grey, and blue atoms represent oxygen, hydrogen, silicon, aluminium, carbon, and nitrogen, respectively.

TABLE 1 Annealing process for developing kerogen surface model.

Ensemble	T (K)	P (bar)	*t* (ns)
NVT	900		0.2
NPT	900	10	0.2
NPT	900→700	10	0.1
NPT	700	10	0.2
NPT	700→500	10	0.1
NPT	500	10	0.2
NPT	500→365	10	0.1
NPT	365	10	0.2
NPT	365	10→275	0.2
NPT	365	275	0.5
NPT	1,000→365	275	1.0
NPT	365	275	1.0

exhibit higher hydrophobicity, while the fully hydroxylated amorphous silica surface display greater hydrophilicity. Jagadisan and Heidari. (2022) conducted MD simulations to explore the influences of thermal maturity and reservoir temperature on the wettability performances of organic kerogen surfaces. Their simulation results indicated that the formed air/water/kerogen contact angle is maximal on type III and minimal on type II kerogen surfaces.Bai et al. (2020) utilized MD simulation to examine the correlation between molecular charge distribution and the efficiency of wettability reversal of quaternary ammonium type cationic surfactants on calcite surfaces. Their results revealed that the charge distribution on the hydrogen atoms within the methylene group of the quaternary ammonium moiety plays a critical role in determining the surfactants' ability to modify wettability. By employing MD simulations, Chen et al. (2015) studied various functional groups on the silica surface. Their results suggested that the presence of different functional groups exhibit a significant impact on the surface contact angle of silica, leading to substantial changes in wettability. Kubelka and his co-workers (Kubelka et al., 2021) investigated the altered wettability of oil-wet calcite by surfactants through MD simulations. They claimed that cationic surfactants demonstrated greater efficiency in separating organic carboxylates and wettability alteration compared to brine.

Although many efforts have been devoted on investigating wettability alteration of oil reservoirs, studies on insightful mechanism and the effects of surfactant type, concentration, and surface properties on wettability of shale reservoirs are still limited. In the present work, we perform MD simulations to investigate the effects of different surfactants and reservoir properties on wettability alteration of shale reservoirs, taking into account their diverse constituents. The obtained results are expected to provide valuable insights and guidance for the development of effective surfactant flooding strategies for enhancing shale oil recovery.

2 Models and simulation methods

2.1 Physical models and force field

In this study, three types of surfaces, i.e., kaolinite, graphene, and kerogen surfaces are constructed to characterize the structures of

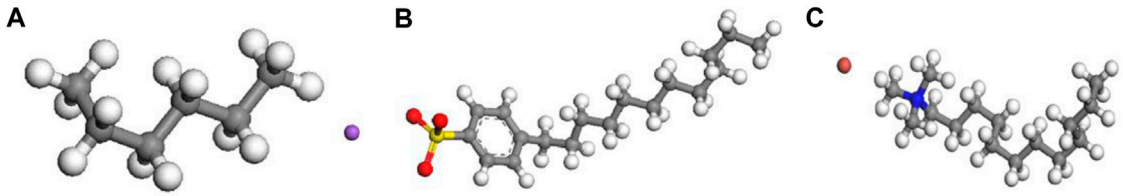

FIGURE 2
Molecular models of **(A)** n-hexane, **(B)** sodium dodecylbenzene sulfonate, and **(C)** dodecyltrimethylammonium bromide. Grey, white, red, yellow, purple, earthy yellow, and blue represent carbon, hydrogen, oxygen, sulphur, sodium, bromine, and nitrogen, respectively.

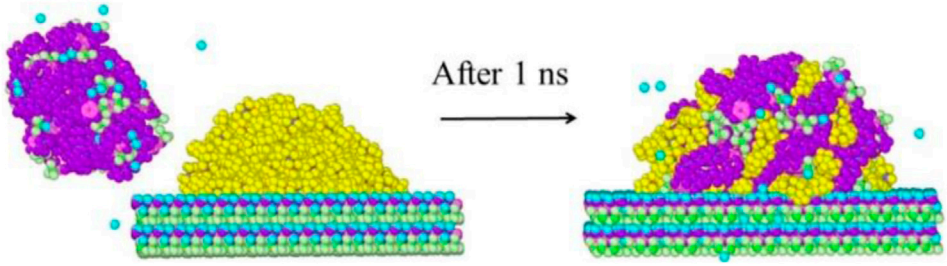

FIGURE 3
Snapshots of the surface/oil/water/surfactant system.

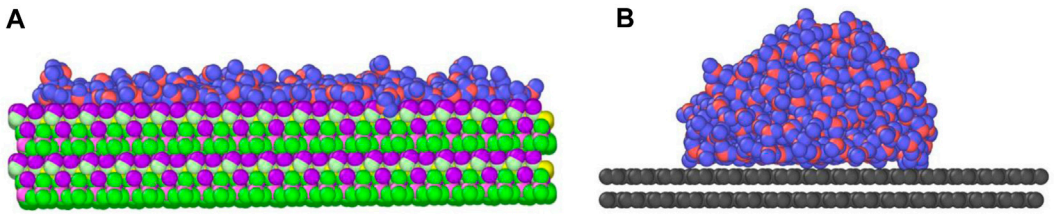

FIGURE 4
Wetting behaviors of water droplet on the **(A)** kaolinite and **(B)** graphene surfaces.

inorganic, simplified organic, and organic surfaces in shale reservoirs, respectively. The Silica-Face-to-Gibbsite-Face (SG-FF) manner is used to construct the {0 0 1} octahedral surface model with dimensions of 81 × 78 × 14 Å^3 of kaolinite, as shown in Figure 1A (Šolc et al., 2011; Tenney and Cygan, 2014; Sun H.-m. et al., 2021). A 33 × 18 × 2 supercell of the graphene unit cell structure with the size of 74 × 77 × 4 Å^3 is built for the graphene surface model, as displayed in Figure 1B. The kerogen surface model is developed based on the relaxation process proposed by Michalec and Lisaĺ (Michalec and Lísal, 2017) and the modification by Yu et al. (2021) Firstly, 40 III-A type kerogen molecules are randomly inserted into a cuboid simulation box with an initial system density of approximately 0.05 g/cm^3. Subsequently, the annealing process is performed following the relaxation protocol outlined in Table 1. After 12 cycles, a kerogen surface model with the size of 63.6 × 63.6 × 22.7 Å^3 is obtained, as presented in Figure 1C. The final density of the model is 1.259 g/cm^3, which is in good agreement with the experimental result of 1.28 ± 0.3 g/cm^3 (Stankiewicz et al., 2015).

In this study, the shale oil model is simplified with n-hexane, as depicted in Figure 2A. The oil molecules are parameterized using the polymer consistent force field (PCFF) (Sun et al., 1994; Plimpton, 1995; Chen et al., 2006; Cui et al., 2022), which has proven to be capable to accurately predict the structural and thermodynamic properties of oil components (Tang et al., 2019). The surfactants utilized in this study are the anionic surfactant sodium dodecylbenzene sulfonate (SDBS) and the cationic surfactant dodecyltrimethylammonium bromide (DTAB), as illustrated in Figures 2B,C. These surfactants are widely used in oil recovery experiments due to their commonality and ready availability. In this study, all molecular models are constructed using the Materials Studio package (version 2017).

2.2 Simulation details

Firstly, 120 n-hexane molecules are randomly placed onto a surface within a simulation box. Following geometrical optimization, the alkane molecules are superimposed on the surface forming an oil droplet. The system is then immersed in water and equilibrated in a canonical (NVT) ensemble at 330 K for 1 ns (Tang et al., 2019). This equilibration stage allows for the determination of the competitive adsorption of oil and water on the surfaces, resulting in different wettability behaviors. After equilibration, water is removed and surfactants are placed on the left side of the system. The water in the simulation is controlled to redissolve the generated shale surface/oil/water/surfactant system. Finally, the shale surface/oil/water/surfactant system is simulated at 330 K for 1 ns, as illustrated in Figure 3. In this work, the time step for the simulations is 1 fs and periodic boundary conditions are adopted (Kubelka et al., 2021). The extended simple point charge (SPC/E) model is used for characterizing water molecules (Taylor et al., 1996). All molecular dynamics simulations in this study are performed on the Large-scale Atomic/Molecular Massively Parallel Simulator (LAMMPS) (Plimpton, 1995). The simulation results are visualized using OVITO software.

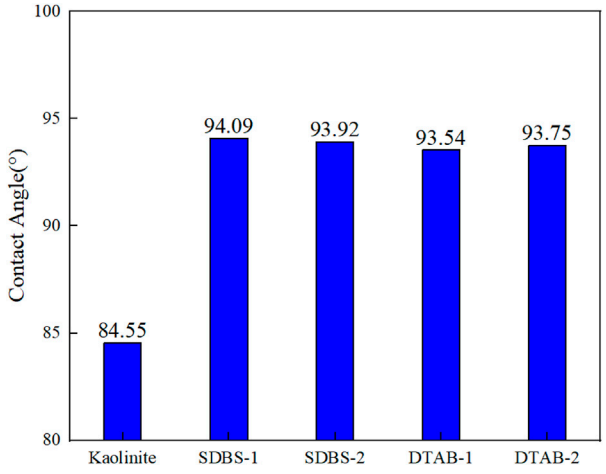

FIGURE 5
Comparison of contact angles on kaolinite surfaces with different surfactants.

3 Results and discussion

3.1 Model validation

In this study, the contact angles of water droplets on the kaolinite and graphite surfaces are first simulated to validate the accuracy of the physical model and force field, as displayed in Figure 4. The simulation results demonstrate that the droplet spreads on the kaolinite surface, forming an incomplete monomolecular layer with a contact angle close to zero. This indicates an extremely hydrophilic nature of kaolinite surface,

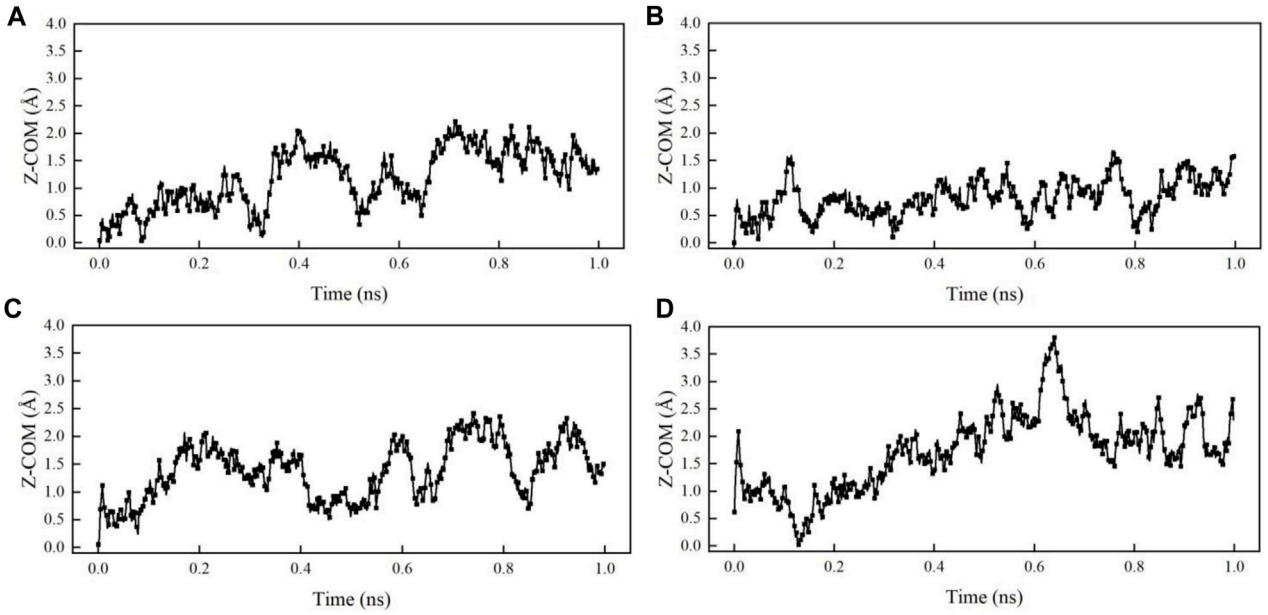

FIGURE 6
Variations of centroid ordinates in different systems: **(A)** SDBS-1; **(B)** SDBS-2; **(C)** DTAB-1; **(D)** DTAB-2.

which is consistent with the results obtained by Šolc et al. (Šolc et al., 2011) The simulated contact angle of water droplet on the graphene surface is 94.2°, which is in good agreement with the simulation result of 99.1° obtained by Xiong et al. (Xiong et al., 2022) In this work, the contact angles of droplets are determined by:

$$\theta = \arcsin\left(\frac{2hr}{h^2 + r^2}\right) \quad (h < R) \tag{1}$$

$$\theta = 90° + \arcsin\left(\frac{2hr}{h^2 + r^2}\right) \quad (h > R) \tag{2}$$

where θ denotes the wetting contact angle, h is the droplet height, r is the radius of the circular contact surface between the droplet and the surface, and R is the radius of the droplet.

3.2 Effect of surfactants on the wettability of inorganic kaolinite surfaces

In order to examine the effects of different types and concentrations of surfactants on the wettability of n-hexane oil droplets on a kaolinite surface, a series of MD simulations are performed. Specifically, two sets surfactants, namely, SDBS-1/DTAB-1 (consisting of 25 surfactant molecules) and SDBS-2/DTAB-2 (consisting of 40 surfactant molecules) are examined.

3.2.1 Comparison of contact angle

To quantitatively describe the contact angles of oil droplets composed of 120 n-hexane molecules on the shale surface, we assume that the oil mass in equilibrium is a part of an ideal sphere. It should be noted that the mentioned contact angles hereinafter are measured with oil droplet on different surfaces.

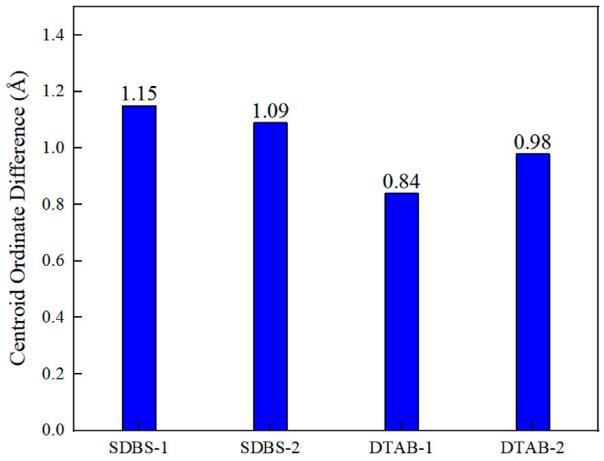

FIGURE 7
Comparison of centroid ordinate differences in different kaolinite systems with different surfactants.

Figure 5 presents the variations in contact angle for the kaolinite/oil/water/surfactant system with different concentrations of SDBS and DTAB. In the SDBS-1 model group, the contact angle of n-hexane oil droplets increases from 84.55° to 94.09° after 1 ns of simulation calculations, while 93.92° for SDBS-2 system. The contact angle increase from 84.55° to 93.54° in DTAB-1 system, while 93.75° for DTAB-2 system. It is concluded that wettability alteration from intermediate-oleophilic to intermediate-oleophobic can be observed for both SDBS and DTAB. However, the concentration of surfactants indicates slight influences on the degree of wettability alteration.

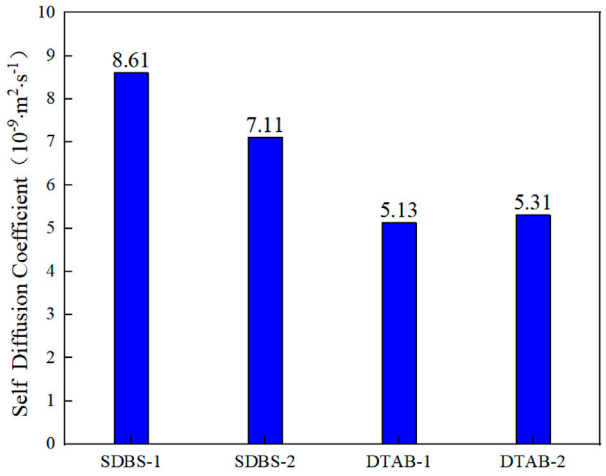

FIGURE 8
Comparison of self-diffusion coefficients in different kaolinite systems with different surfactants.

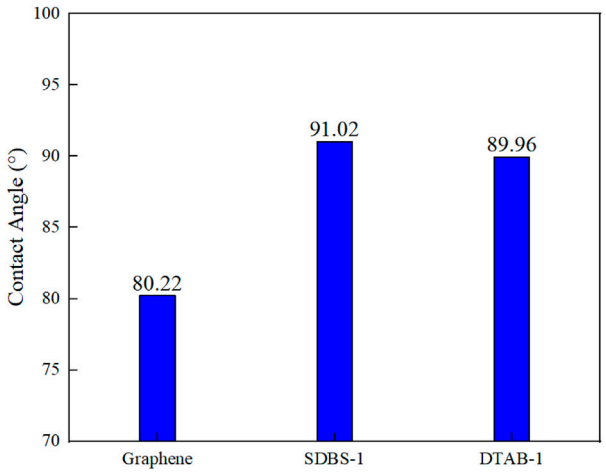

FIGURE 9
Comparison of contact angle on different graphene surfaces with different surfactants.

3.2.2 Comparison of centroid ordinates

The vertical distance between the centroid of the oil droplet and kaolinite surface, i.e., the centroid ordinates of the oil droplet, is calculated by the COM (centre of mass) command in LAMMPS, and the centroid ordinates of the oil droplets in the Z direction are recorded every 2000 steps to observe the trend of oil droplets. Figure 6 shows the comparison of centroid ordinate differences in kaolinite system. The rise in the centroid ordinates indicates that the oil droplets have a tendency to move upwards away from the kaolinite surface due to the action of the surfactant. After 1 ns of simulation, the centroid ordinates of n-hexane oil droplets in SDBS-1 system increases by 1.15 Å, while 1.09 Å for SDBS-2 system. The COM trajectory of DTAB-1 system with the cationic surfactant also shows that the volume of oil droplet increases after the addition of DTAB, and the centroid ordinate in the Z direction rises by 0.84 Å. The centroid ordinates increase by 0.98 Å in the DTAB-2 system, as can be seen in Figure 7. It can be observed that n-hexane aggregates move much faster in the Z direction due to the interaction with SDBS. However, this effect decreases with the increasing concentration. Under the action of DTAB, the aggregates move faster with higher concentrations.

3.2.3 Comparison of self-diffusion coefficients

The self-diffusion coefficient can fully reflect the diffusion and migration ability of n-hexane molecules on the shale surface. The self-diffusion coefficient of n-hexane molecules needs to be calculated to describe their movement and changes on the shale surface. The calculation formula can be written as:

$$MSD = \langle |R(t) - R(0)|^2 \rangle \tag{3}$$

$$D = \frac{1}{2N} \lim_{t\to\infty} \frac{d}{dt} \langle |R(t) - R(0)|^2 \rangle \tag{4}$$

where D is the self-diffusion coefficient of the n-hexane molecule, $R(t)$ is the position of the n-hexane molecule at time t, and $R(0)$ is the initial position of the n-hexane molecule. First, the mean square displacement of n-hexane molecules is obtained using the MSD command in LAMMPS. Then, the self-diffusion coefficient can be calculated.

Figure 8 shows the comparison of self-diffusion coefficients of the oil droplets. The self-diffusion coefficient of oil droplets in the SDBS-1 and SDBS-2 model are 8.61×10^{-9} and 7.11×10^{-9} $m^2 \cdot s^{-1}$, respectively. The self-diffusion coefficients in the DTAB-1 and

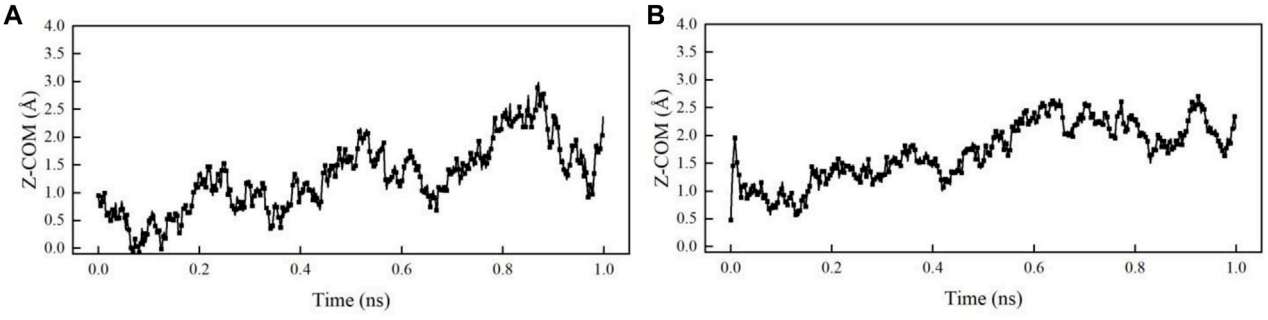

FIGURE 10
Variations of centroid ordinates in the systems: **(A)** SDBS-1; **(B)** DTAB-1.

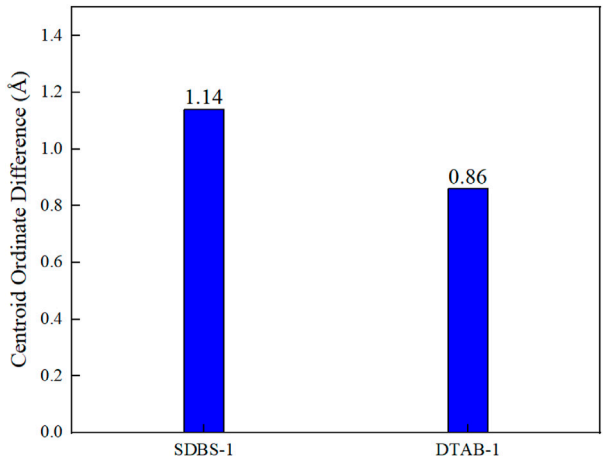

FIGURE 11
Comparison of centroid ordinate variations in different graphene systems with different surfactants.

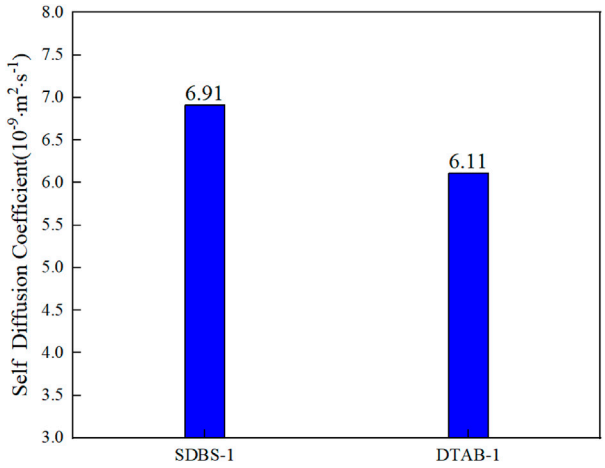

FIGURE 12
Comparison of self-diffusion coefficients in different graphene systems with different surfactants.

DTAB-2systems are 5.13×10^{-9} and 5.31×10^{-9} m$^2 \cdot$ s^{-1}, respectively. It indicates that the n-hexane aggregates diffuse to a greater extent due to the action of SDBS. Higher SDBS concentrations lead to smaller self-diffusion coefficients of n-hexane molecules. In contrast, the higher concentration in the DTAB group corresponds to a greater self-diffusion coefficient. With higher self-diffusion coefficients, oil molecules have greater movement speed, stronger escape ability, and easier detachment from the kaolinite surface.

The magnitudes of contact angle and self-diffusion coefficient and the centroid position variation of the oil droplets clearly indicate the different effects of different surfactants on the oil adsorption onto the kaolinite surface. According to the simulation results, SDBS has better oil displacement performance than DTAB. This difference in oil displacement performance of the two surfactants was attributed to the head group effect. The groups in SDBS have a stronger attraction for water molecules. As a result, the SDBS migrates faster over the oil aggregation surface, and the oil molecule deformation separation is faster.

Although the data are somewhat scattered, a clear correlation between the wettability index and surfactant concentration can be observed. At higher concentrations, SDBS has less effect on the wettability variation of oil droplets on the kaolinite surface and less wettability inversion effect. Meanwhile, DTAB shows the opposite trend. Therefore, the effect of DTAB is opposite to that of SDBS. At higher concentrations, DTAB has a better effect on the wettability variation of oil droplets on the kaolinite surface and a better wettability inversion effect.

3.3 Effect of surfactants on the wettability of graphene surfaces

In the section, the effects of surfactant on the wettability on the simplified graphene surfaces are focused. We develop the system models containing 25 surfactant molecules, denoted as SDBS-1 and DTAB-1, respectively. After 1 ns of simulation, the contact angle of n-hexane oil droplets in SDBS-1 increases from 80.22° to 91.02°, while that in DTAB-1 increases to 89.96°, as shown in Figure 9. The vertical distances between the centroid of the oil droplet and the graphene surface, i.e., the centroid ordinates of the oil droplet, are recorded every 2000 steps to observe the trend of the oil droplets, as shown in Figure 10.

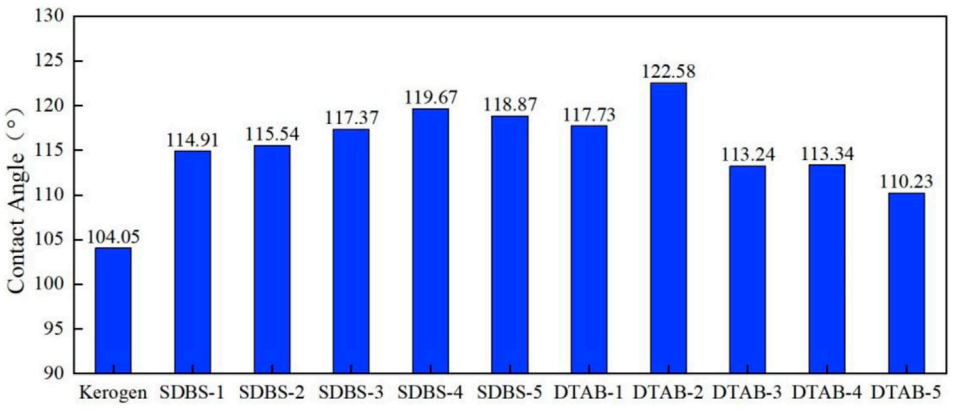

FIGURE 13
Comparison of contact angles on kerogen surfaces with different surfactants.

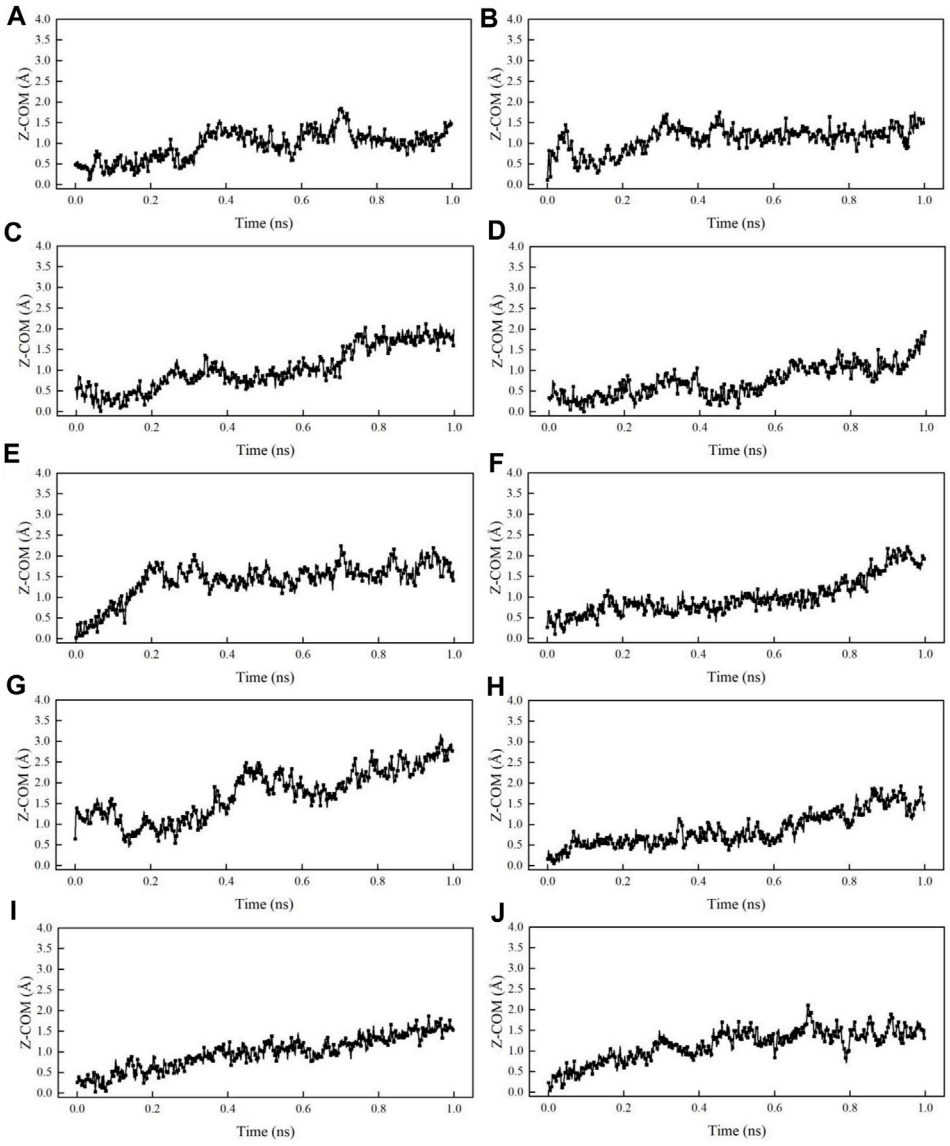

FIGURE 14
Variations of centroid ordinates in different systems: **(A)** SDBS-1; **(B)** SDBS-2; **(C)** SDBS-3; **(D)** SDBS-4; **(E)** SDBS-5; **(F)** DTAB-1; **(G)** DTAB-2; **(H)** DTAB-3; **(I)** DTAB-4; **(J)** DTAB-5.

After 1 ns of simulation calculation, the centroid ordinate of n-hexane oil droplets rises by 1.14 Å in SDBS-1 and 0.86 Å in DTSB-1, as shown in Figure 11. The diffusion coefficient can fully reflect the diffusion and migration ability of n-hexane molecules on the shale surface. The diffusion coefficient of n-hexane molecules needs to be calculated to describe their movement and changes on the shale surface. As shown in Figure 12, the diffusion coefficient is 6.91×10^{-9} $m^2 \cdot s^{-1}$ in SDBS-1 and 6.11×10^{-9} $m^2 \cdot s^{-1}$ in DTAB-1. The magnitudes of contact angle and diffusion coefficient and the centroid position variation of the oil droplets clearly indicate that the surfactants can alter the wettability of oil adsorbed onto the graphene surface. Meanwhile, the effect of SDBS is better than DTAB, which is consistent with the findings in the previous section. The reason may be that groups in SDBS have a stronger attraction for water molecules. As a result, the SDBS migrates faster over the oil aggregation surface, and the oil molecule deformation separation is faster. We can all see that SDBS is more effective than DTAB when compared to kaolinite systems with the same number of surfactants, but SDBS is slightly less effective in changing wettability in the graphene system than in the kaolinite system. DTAB, on the other hand, demonstrated the inverse trend, with a slightly better effect in the graphene system than in the kaolinite system. This could be due to the various properties of the shale surface.

3.4 Effect of surfactants on the wettability of kerogen surfaces

To examine the effects of surfactant on wettability alteration of organic matter in shale reservoirs, a realistic kerogen surface is also developed. Different surfactant concentrations of SDBS-1 and

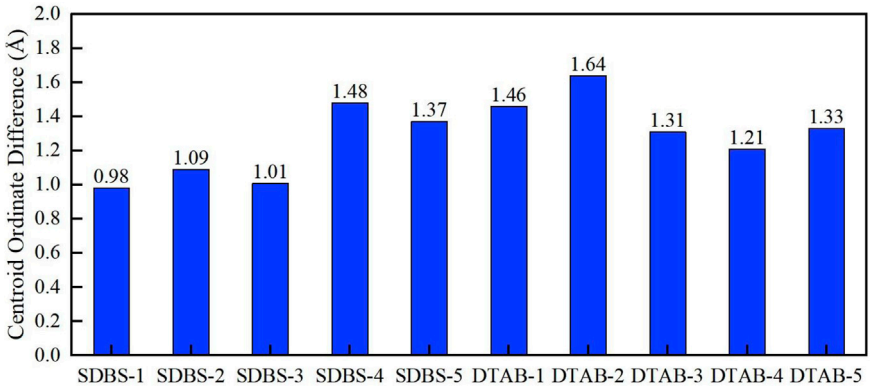

FIGURE 15
Comparison of centroid ordinate differences in different kerogen systems with different surfactants.

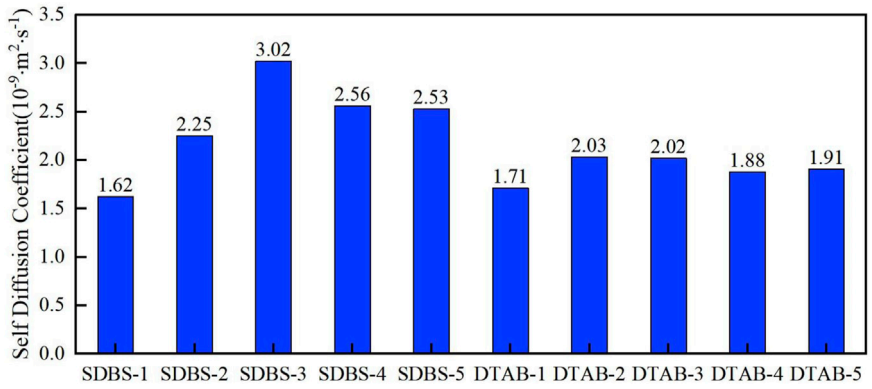

FIGURE 16
Comparison of self-diffusion coefficients in different kerogen systems with different surfactants.

DTAB-1 to SDBS-5 and DTAB-5 (20, 25, 30, 35, 40 surfactant molecules) are further designed.

3.4.1 Comparison of contact angles

Figure 13 shows the contact angle variation of the kerogen/oil/water/surfactant system with different concentrations of SDBS or DTAB. Without surfactant, the contact angle of the equilibrated oil droplet is 104.05°on the kerogen surface. With the increase of SDBS concentration, the contact angle of oil droplet increases from 114.91° to 119.67° and then shows a slight decrease to 118.87°. While for DTAB, a similar tendency is observed, with the contact angle increasing from 117.73° to 122.58° and declining to 110.23°. It indicates that there is an optimal concentration of surfactant for wettability alteration. It can be observed from Figure 13 that with 25 surfactant molecules, the interaction between DTAB and the oil/water interface is more intense, and the contact angle of n-hexane oil droplets changes more rapidly. While for SDBS, the contact angle changes more drastically with 35 surfactant molecules.

3.4.2 Comparison of centroid ordinates

Figure 14 shows the comparison of centroid ordinate differences in all kerogen systems. After 1 ns of calculation, the centroid ordinates of oil droplets in the system with SDBS increase by 0.98, 1.09, 1.01, 1.48 and 1.37 Å, respectively. The trajectory of the DTAB system also shows that the centroid ordinates in the Z direction increase by 1.46, 1.64, 1.31, 1.21 and 1.33 Å, respectively. Figure 15 shows a comparison of oil droplet centroid ordinate variations along the vertical direction. It is observed that the droplet move much faster in Z direction due to the interaction with DTAB. It is clear from the figure that there are optimal concentrations for both SDBS and DTAB in altering wettability of kerogen surface. The variation pattern of oil droplet centroid is consistent with that of contact angle.

3.4.3 Comparison of self-diffusion coefficients

Figure 16 shows the comparison of self-diffusion coefficients of oil droplets. It is found that the self-diffusion coefficients of oil

molecules increases and then decreases with the increment of the concentrations of SDBS and DTAB, which are consistent with earlier findings. It is observed that the effects of surfactant on the wettability of organic kerogen surfaces is significantly different from that on inorganic kaolinite surfaces. The difference is due to the different nature of the substrate. Different types of surfactants have different effects on the solution surface/interfacial tension. Surfactants significantly decrease the interfacial tension, but the extents of the decreases vary. As a water-bearing aluminosilicate, kaolinite is a clay mineral. Kerogen is a dispersed organic matter in sedimentary rocks insoluble in alkalis, non-oxidizing acids, and organic solvents. The differences in the structure and properties of kaolinite and kerogen lead to different effects of surfactants on their surfaces.

4 Conclusion

In the present work, molecular dynamics simulations have been adopted to investigate the effects of surfactant on wettability alterations on kaolinite, graphene, and kerogen surfaces in shale reservoirs. The following conclusions can be drawn.

(1) The changes of contact angle, centroid ordinates, and self-diffusion coefficients in the simulations indicate that surfactants can alter the wettability of oil droplets on the surfaces of kaolinite, graphene, and kerogen.
(2) For oil-wet kaolinite surfaces with contact angle of 84.55°, the wettability reversals have been observed for both SDBS and DTAB. However, compared with graphene and kerogen surfaces, the degree of wettability alteration is less sensitive to surfactant concentration.
(3) For organic graphene and kerogen surfaces, surfactants are found to be able to further improve the contact angels of oil droplets. However, for kerogen surfaces, there is an optimal surfactant concentration for both SDBS and DTAB, beyond which the further addition of surfactant could decrease the contact angel.
(4) The obtained results suggest that the effects of SDBS and DTAB on the surfaces of kaolinite, graphene, and kerogen are obviously different, which is due to the interactions between headgroups of surfactants and surfaces.

Data availability statement

The original contributions presented in the study are included in the article/Supplementary Material, further inquiries can be directed to the corresponding authors.

Author contributions

DK: Funding acquisition, Investigation, Project administration, Validation, Writing–review and editing. XM: Conceptualization, Data curation, Validation, Writing–review and editing. JZ: Data curation, Investigation, Visualization, Writing–original draft, WZ: Validation, Visualization, Writing–original draft, Writing–review and editing.

Acknowledgments

The authors acknowledge the financial support from the Natural Sciences for Youth Foundation of China (No. 42102163), the Fundamental Research Funds of the Central Universities (No. FRF-TP-20-006A1) and the Open Fund of State Key Laboratory of Shale Oil and Gas Enrichment Mechanisms and Effective Development (No. 33550000-21-FW2099-0166).

Conflict of interest

The authors declare that the research was conducted in the absence of any commercial or financial relationships that could be construed as a potential conflict of interest.

Publisher's note

References

Afekare, D., Garno, J., and Rao, D. (2021). Enhancing oil recovery using silica nanoparticles: nanoscale wettability alteration effects and implications for shale oil recovery. *J. Petrol. Sci. Eng.* 203, 108897. doi:10.1016/j.petrol.2021.108897

Al Mahrouqi, D., Vinogradov, J., and Jackson, M. D. (2017). Zeta potential of artificial and natural calcite in aqueous solution. *Adv. Colloid Interface Sci.* 240, 60–76. doi:10.1016/j.cis.2016.12.006

Bai, S., Kubelka, J., and Piri, M. (2020). Relationship between molecular charge distribution and wettability reversal efficiency of cationic surfactants on calcite surfaces. *J. Mol. Liq.* 318, 114009. doi:10.1016/j.molliq.2020.114009

Chai, J., Liu, S., and Yang, X. (2009). Molecular dynamics simulation of wetting on modified amorphous silica surface. *Appl. Surf. Sci.* 255, 9078–9084. doi:10.1016/j.apsusc.2009.06.109

Chen, C., Zhang, N., Li, W., and Song, Y. (2015). Water contact angle dependence with hydroxyl functional groups on silica surfaces under CO_2 sequestration conditions. *Environ. Sci. Technol.* 49, 14680–14687. doi:10.1021/acs.est.5b03646

Chen, Y.-J., Xu, G.-Y., Yuan, S.-L., and Sun, H.-Y. (2006). Molecular dynamics simulations of AOT at isooctane/water interface. *Colloid Surf. A* 273, 174–178. doi:10.1016/j.colsurfa.2005.08.031

Chen, Z., Sun, J., Wu, P., Liu, W., Chen, C., Lang, C., et al. (2023). Cyclodextrin as a green anti-agglomerant agent in oil–water emulsion containing asphalt. *Fuel* 335, 127041. doi:10.1016/j.fuel.2022.127041

Cui, F., Jin, X., Liu, H., Wu, H., and Wang, F. (2022). Molecular modeling on Gulong shale oil and wettability of reservoir matrix. *Capillarity* 5 (4), 65–74. doi:10.46690/capi.2022.04.01

Dang, W., Nie, H., Zhang, J., Tang, X., Jiang, S., Wei, X., et al. (2022). Pore-scale mechanisms and characterization of light oil storage in shale nanopores: new method and insights. *Geosci. Front.* 13, 101424. doi:10.1016/j.gsf.2022.101424

Deng, X., Kamal, M. S., Patil, S., Hussain, S. M. S., and Zhou, X. (2020). A review on wettability alteration in carbonate rocks: wettability modifiers. *Energy fuels.* 34, 31–54. doi:10.1021/acs.energyfuels.9b03409

Guo, H., He, M., Sun, C., Li, B., and Zhang, F. (2012). Hydrophilic and strength-softening characteristics of calcareous shale in deep mines. *J. Rock Mech. Geotech. Eng.* 4, 344–351. doi:10.3724/sp.j.1235.2012.00344

Guo, Q., Yao, Y., Hou, L., Tang, S., Pan, S., and Yang, F. (2022). Oil migration, retention, and differential accumulation in "sandwiched" lacustrine shale oil systems from the Chang 7 member of the Upper Triassic Yanchang Formation, Ordos Basin, China. *Int. J. Coal Geol.* 261, 104077. doi:10.1016/j.coal.2022.104077

Jagadisan, A., and Heidari, Z. (2022). Molecular dynamic simulation of the impact of thermal maturity and reservoir temperature on the contact angle and wettability of kerogen. *Fuel* 309, 122039. doi:10.1016/j.fuel.2021.122039

Kubelka, J., Bai, S., and Piri, M. (2021). Effects of surfactant charge and molecular structure on wettability alteration of calcite: insights from molecular dynamics simulations. *J. Phys. Chem. B* 125, 1293–1305. doi:10.1021/acs.jpcb.0c10361

Larestani, A., Mousavi, S. P., Hadavimoghaddam, F., Ostadhassan, M., and Hemmati-Sarapardeh, A. (2022). Predicting the surfactant-polymer flooding performance in chemical enhanced oil recovery: cascade neural network and gradient boosting decision tree. *Alexandria Eng. J.* 61, 7715–7731. doi:10.1016/j.aej.2022.01.023

Liu, J., Sheng, J. J., and Huang, W. (2019b). Experimental investigation of microscopic mechanisms of surfactant-enhanced spontaneous imbibition in shale cores. *Energy fuels.* 33, 7188–7199. doi:10.1021/acs.energyfuels.9b01324

Liu, J., Sheng, J. J., Wang, X., Ge, H., and Yao, E. (2019a). Experimental study of wettability alteration and spontaneous imbibition in Chinese shale oil reservoirs using anionic and nonionic surfactants. *J. Petrol. Sci. Eng.* 175, 624–633. doi:10.1016/j.petrol.2019.01.003

Liu, X., Kang, Y., Yan, L., Tian, J., Li, J., and You, L. (2022). Implication of interfacial tension reduction and wettability alteration by surfactant on enhanced oil recovery in tight oil reservoirs. *Energy Rep.* 8, 13672–13681. doi:10.1016/j.egyr.2022.10.052

Michalec, L., and Lísal, M. (2017). Molecular simulation of shale gas adsorption onto overmature type II model kerogen with control microporosity. *Mol. Phys.* 115, 1086–1103. doi:10.1080/00268976.2016.1243739

Mirchi, V., Saraji, S., Goual, L., and Piri, M. (2015). Dynamic interfacial tension and wettability of shale in the presence of surfactants at reservoir conditions. *Fuel* 148, 127–138. doi:10.1016/j.fuel.2015.01.077

Okunade, O. A., Yekeen, N., Padmanabhan, E., Al-Yaseri, A., Idris, A. K., and Khan, J. A. (2021). Shale core wettability alteration, foam and emulsion stabilization by surfactant: impact of surfactant concentration, rock surface roughness and nanoparticles. *J. Petrol. Sci. Eng.* 207, 109139. doi:10.1016/j.petrol.2021.109139

Pei, H., Zhang, G., Ge, J., Tang, M., and Zheng, Y. (2012). Comparative effectiveness of alkaline flooding and alkaline–surfactant flooding for improved heavy-oil recovery. *Energy fuels.* 26, 2911–2919. doi:10.1021/ef300206u

Plimpton, S. (1995). Fast Parallel algorithms for short-range molecular dynamics. *J. Comput. Phys.* 117, 1–19. doi:10.1006/jcph.1995.1039

Qin, C., Jiang, Y., Zhou, J., Zuo, S., Chen, S., Liu, Z., et al. (2022). Influence of supercritical CO2 exposure on water wettability of shale: implications for co2 sequestration and shale gas recovery. *Energy* 242, 122551. doi:10.1016/j.energy.2021.122551

Rezaei, N., Zendehboudi, S., Chatzis, I., and Lohi, A. (2018). Combined benefits of capillary barrier and injection pressure control to improve fluid recovery at breakthrough upon gas injection: an experimental study. *Fuel* 211, 638–648. doi:10.1016/j.fuel.2017.09.048

Roshan, H., Al-Yaseri, A. Z., Sarmadivaleh, M., and Iglauer, S. (2016). On wettability of shale rocks. *J. Colloid Interface Sci.* 475, 104–111. doi:10.1016/j.jcis.2016.04.041

SalahEldin Hussien, O., Elraies, K. A., Almansour, A., Husin, H., Belhaj, A., and Ern, L. (2019). Experimental study on the use of surfactant as a fracking fluid additive for improving shale gas productivity. *J. Petrol. Sci. Eng.* 183, 106426. doi:10.1016/j.petrol.2019.106426

Shi, K., Chen, J., Pang, X., Jiang, F., Hui, S., Pang, H., et al. (2022). Effect of wettability of shale on CO2 sequestration with enhanced gas recovery in shale reservoir: implications from molecular dynamics simulation. *J. Nat. Gas. Sci. Eng.* 107, 104798. doi:10.1016/j.jngse.2022.104798

Šolc, R., Gerzabek, M. H., Lischka, H., and Tunega, D. (2011). Wettability of kaolinite (001) surfaces — molecular dynamic study. *Geoderma* 169, 47–54. doi:10.1016/j.geoderma.2011.02.004

Stankiewicz, A., Bennett, B., Wint, O., Ionkina, N., Motherwell, B., and Mastalerz, M. (2015). "Kerogen density revisited – lessons from the duvernay shale," in Unconventional Resources Technology Conference, San Antonio, Texas, 20-22 July 2015, 864–874. doi:10.15530/urtec-2015-2157904

Su, S., Jiang, Z., Shan, X., Zhu, Y., Wang, P., Luo, X., et al. (2018). The wettability of shale by NMR measurements and its controlling factors. *J. Petrol. Sci. Eng.* 169, 309–316. doi:10.1016/j.petrol.2018.05.067

Sun, C., Nie, H., Dang, W., Chen, Q., Zhang, G., Li, W., et al. (2021a). Shale gas exploration and development in China: current status, geological challenges, and future directions. *Energy fuels.* 35, 6359–6379. doi:10.1021/acs.energyfuels.0c04131

Sun, H.-m., Yang, W., Chen, R.-p., and Kang, X. (2021c). Microfabric characteristics of kaolinite flocculates and aggregates — insights from large-scale molecular dynamics simulations. *Appl. Clay Sci.* 206, 106073. doi:10.1016/j.clay.2021.106073

Sun, H., Mumby, S. J., Maple, J. R., and Hagler, A. T. (1994). An *ab initio* CFF93 all-atom force field for polycarbonates. *J. Am. Chem. Soc.* 116, 2978–2987. doi:10.1021/ja00086a030

Sun, J., Chen, Z., Wang, X., Zhang, Y., Qin, Y., Chen, C., et al. (2023). Displacement characteristics of CO_2 to CH_4 in heterogeneous surface slit pores. *Energy fuels.* 37, 2926–2944. doi:10.1021/acs.energyfuels.2c03610

Sun, Y.-P., Xin, Y., Lyu, F.-T., and Dai, C.-L. (2021b). Experimental study on the mechanism of adsorption-improved imbibition in oil-wet tight sandstone by a nonionic surfactant for enhanced oil recovery. *Pet. Sci.* 18, 1115–1126. doi:10.1016/j.petsci.2021.07.005

Tang, L., Song, Y., Jiang, S., Li, L., Li, Z., Li, Q., et al. (2020). Sealing mechanism of the roof and floor for the wufeng-longmaxi shale gas in the southern sichuan basin. *Energy fuels.* 34, 6999–7018. doi:10.1021/acs.energyfuels.0c00983

Tang, X., Xiao, S., Lei, Q., Yuan, L., Peng, B., He, L., et al. (2019). Molecular dynamics simulation of surfactant flooding driven oil-detachment in nano-silica channels. *J. Phys. Chem. B* 123, 277–288. doi:10.1021/acs.jpcb.8b09777

Taylor, R. S., Dang, L. X., and Garrett, B. C. (1996). Molecular dynamics simulations of the liquid/vapor interface of SPC/E water. *J. Phys. Chem.* 100, 11720–11725. doi:10.1021/jp960615b

Tenney, C. M., and Cygan, R. T. (2014). Molecular simulation of carbon dioxide, brine, and clay mineral interactions and determination of contact angles. *Environ. Sci. Technol.* 48, 2035–2042. doi:10.1021/es404075k

Xiong, J., Tang, J., Zhou, X., Liu, X., Liang, L., and Hou, L. (2022). Molecular dynamics simulation and experimental studies of the wettability behaviors of shales. *Energy fuels.* 36, 3526–3538. doi:10.1021/acs.energyfuels.1c04346

Yang, N., Yuan, R., Li, W., Tan, X., Liu, Z., Zhang, Q., et al. (2023). Magnetic-driving giant multilayer polyelectrolyte microcapsules for intelligent enhanced oil recovery. *Colloid Surf. A* 664, 131107. doi:10.1016/j.colsurfa.2023.131107

Yao, Y., Wei, M., and Kang, W. (2021). A review of wettability alteration using surfactants in carbonate reservoirs. *Adv. Colloid Interface Sci.* 294, 102477. doi:10.1016/j.cis.2021.102477

Yu, K. B., Bowers, G. M., Loganathan, N., Kalinichev, A. G., and Yazaydin, A. O. (2021). Diffusion behavior of methane in 3D kerogen models. *Energy fuels.* 35, 16515–16526. doi:10.1021/acs.energyfuels.1c02167

Zhang, H., Dong, M., and Zhao, S. (2010). *Energy fuels.* 24, 1829–1836. doi:10.1021/ef901310v

Zhang, L., Liao, H., and Cui, M. (2022). Effect of CO2 flooding in an oil reservoir with strong bottom-water drive in the Tahe Oilfield, Tarim Basin, Northwest China. *Energy Geosci.*, 100127. doi:10.1016/j.engeos.2022.08.004

Zhang, W., Huang, Z., Li, X., Chen, J., Guo, X., Pan, Y., et al. (2020). Estimation of organic and inorganic porosity in shale by NMR method, insights from marine shales with different maturities. *J. Nat. Gas. Sci. Eng.* 78, 103290. doi:10.1016/j.jngse.2020.103290

Zhao, M., Guo, X., Wu, Y., Dai, C., Gao, M., Yan, R., et al. (2021). Development, performance evaluation and enhanced oil recovery regulations of a zwitterionic viscoelastic surfactant fracturing-flooding system. *Colloid Surf. A* 630, 127568. doi:10.1016/j.colsurfa.2021.127568

Zhao, Y., and Jin, Z. (2021). Hydrocarbon mixture phase behavior in multi-scale systems in relation to shale oil recovery: the effect of pore size distributions. *Fuel* 291, 120141. doi:10.1016/j.fuel.2021.120141

Zheng, J., Feng, G., Ren, Z., Qi, N., Coffman, D. M., Zhou, Y., et al. (2022). China's energy consumption and economic activity at the regional level. *Energy* 259, 124948. doi:10.1016/j.energy.2022.124948

Zhou, W., Jiang, L., Liu, X., Hu, Y., and Yan, Y. (2022). Molecular insights into the effect of anionic-nonionic and cationic surfactant mixtures on interfacial properties of oil-water interface. *Colloid Surf. A* 637, 128259. doi:10.1016/j.colsurfa.2022.128259

Zhou, W., Wang, H., Yan, Y., and Liu, X. (2019a). Adsorption mechanism of CO_2/CH_4 in kaolinite clay: insight from molecular simulation. *Energy & Fuels* 33, 6542–6551. doi:10.1021/acs.energyfuels.9b00539

Zhou, W., Wang, H., Yang, X., Liu, X., and Yan, Y. (2020). Confinement effects and CO_2/CH_4 competitive adsorption in realistic shale kerogen nanopores. *Ind. Eng. Chem. Res.* 59, 6696–6706. doi:10.1021/acs.iecr.9b06549

Zhou, W., Wang, H., Zhang, Z., Chen, H., and Liu, X. (2019b). Molecular simulation of CO_2/CH_4/H_2O competitive adsorption and diffusion in brown coal. *RSC Adv.* 9, 3004–3011. doi:10.1039/c8ra10243k

Zou, C., Zhu, R., Chen, Z.-Q., Ogg, J. G., Wu, S., Dong, D., et al. (2019). Organic-matter-rich shales of China. *Earth Sci. Rev.* 189, 51–78. doi:10.1016/j.earscirev.2018.12.002